Characteristics Portrayal of Nano $Ce_xM_yO_{1-x+y}$ (M = Zn, Mg & Ni)

Suriakala PERUMAL RAJA [1]*, Tamilarasan KARPPUSAMY [2]

[1] *Department of Physics, Rajapalayam Rajus' College, Rajapalayam, 626117, Tamil Nadu, India*
[2] *Department of Physics, Kongu Engineering College, Perundurai, 638052, Erode, Tamil Nadu, India*

crossref http://dx.doi.org/10.5755/j01.ms.22.2.7048

Received 06 May 2014; accepted 19 February 2015

Nano $Ce_xM_yO_{1-x+y}$ (M = Zn, Mg and Ni) materials were prepared for the applications of spintronic devices by microwave induced combustion process using cerium nitrate, zinc nitrate, magnesium nitrate and nickel nitrate as a starting materials and sorbitol and glycine used as a fixed ratio of fuel. The structural properties of all samples were analyzed by XRD, SEM and TEM. The crystallite size was found in the nano ranges in the order of 27 nm to 3 nm and their lattice parameters are in the range of 5.3739A˚ to 5.4479A˚. These structural parameters are affected by amount of fuel ratio, nature of materials integrated and preparation method. The optical properties were examined via UV-Vis spectroscopy. The variation of the band gap energy was due to concentration of the grain boundaries, which depends on the type of mixing materials. The magnetic nature of the prepared samples was studied by Vibration Sample Magnetometer (VSM). The VSM results show the existence of weak ferromagnetic and paramagnetic nature of ceria nanocrystallite materials which is also depending on the incorporation of various materials.
Keywords: ceria based materials, structural properties, optical properties, magnetic properties.

1. INTRODUCTION

Dilute magnetic semiconductor materials have become very interesting nowadays, especially for spintronic applications. Unlike dilute magnetic semiconductors, ceria has cubic structure that will facilitate the integration of spintronic devices with advanced silicon microelectronic devices. In this respect, ceria attracts great attention since it has a high dielectric constant ($\varepsilon = 26$). The general semiconducting behavior of some wide bandgap materials such as CeO_2 is found to be ferromagnetic dielectrics/insulators. Hence, systematic studies of the magnetic properties in these magnetic dielectrics are needed in order to understand the mechanism responsible for ferromagnetic interactions. It has recently gained much attention due to their potential use in several technological applications such as drug delivery [1], catalysis [2], and fuel cells [3]. Ceria in nanocrystalline phase has become feasible now, and as a result, the drastic change in its properties like structural [4], optical [5], and magnetic [6] properties with varying particle sizes have created renewed interest in this material. Nanocrystalline ceria has been used as a sun screen material for its outstanding ultraviolet absorption property [7]. Ceria has an extensive significant outlook in electronic spin devices due to its ferromagnetic nature. Dilute magnetic dielectric ceria has been influenced and enhanced spintronic capabilities [8]. The magnetic properties of ceria can be varied by its size, added with other materials and also preparation methods [9]. The origins of the ferromagnetic of ceria is mainly due to oxygen vacancies, doping magnetic ions, Ce^{3+}/Ce^{4+} pairs on surface, cerium vacancies, consistence of Ce^{3+} on surface, size of grains [10]. Room-temperature ferromagnetism has been observed in the nanoparticles of ceria based materials [11]. The ferromagnetism in Co-doped ceria not only depends on the doping concentration of transition element, but also on the microstructure of film, including its crystallization, defects, vacancies, etc [12]. The same behavior was observed in Fe doped ceria prepared by sol gel technique. Nano crystalline magnesium cerium gadolinium ferrite was prepared through sol-gel route having saturation magnetization of Gd^{3+} Ce^{3+} substituted Mg ferrites is higher than unsubstituted ferrite [13]. Magnetic property study of nickel cerium doped zinc ferrite nano particles was prepared by sol-gel auto combustion route [14]. The aim of the present work is to prepare ceria based materials that are characterized by significant properties needed in many applications.

2. EXPERIMENTAL DETAILS

All the reagents used for the preparation were analytically pure. Chemicals like cerium nitrate $Ce(NO_3)_3{\cdot}6H_2O$, zinc nitrate $Zn(NO_3)_2{\cdot}6H_2O$, magnesium nitrate $Mg(NO_3)_2{\cdot}6H_2O$ and nickel nitrate $Ni(NO_3)_2{\cdot}6H_2O$ act as precursor materials and glycine and sorbitol act as fuels. The stock solution of 0.25 mole, 0.75 mole of $Ce(NO_3)_3{\cdot}6H_2O$, 0.25 M of $Zn(NO_3)_2{\cdot}6H_2O$, $Mg(NO_3)_2{\cdot}6H_2O$, $Ni(NO_3)_2{\cdot}6H_2O$ and 0.5mole of glycine were prepared using de-ionised water in advance and stored at room temperature. 100 ml of $Ce(NO_3)_3{\cdot}6H_2O$,100 ml of doped nitrate, 4 ml of glycine and 4 ml of sorbitol were mixed in the beaker. The mixed solution was heated at 250 °C for 10 min and applied microwave power at 300 W for 8 min, a lot of fumes were observed. The final products were named as CEA for 0.25 mole of cerium nitrate, CEC for 0.75 mole of cerium nitrate, CZA for 0.25 mole of cerium nitrate and 0.25 mole of zinc nitrate, CZC for 0.75mole of cerium nitrate and 0.25 mole of zinc nitrate, CMA for 0.25 mole of cerium nitrate and 0.25 mole of magnesium nitrate, CMC for 0.75 mole of cerium nitrate and 0.25 mole of magnesium nitrate, CNA for 0.25 mole of

* Corresponding author. Tel.: 9150153225; fax: 04563226467.
Email address: *psuriakala@gmail.com* (S. Perumal Raja)

cerium nitrate and 0.25 mole of nickel nitrate and CNC for 0.75 mole of cerium nitrate and 0.25 mole of nickel nitrate.

The X-ray diffraction (XRD) patterns of the powder samples were measured at room temperature with BrukerAxs Ds Advance diffractrometer with CuKα radiation of wavelength 1.5418 Å. Optical properties of nickel doped ceria powder was studied by UV-Vis – NIR Spectrophotometer (Varian, Cary 5000). Surface morphology of the powders was studied using Scanning Electron Microscope JEOL Model JSM - 6390LV EDS JEOL Model JED – 2300 and TEM JEOL JEM 2100 High Resolution Transmission Electron Microscope (HRTEM) were used for morphology of the material. Magnetic properties were determined using Vibrating Sample Magnetometer (VSM) LAKESHORE VSM 7410.

3. RESULTS AND DISCUSSION

Ceria exhibit a face centered cubic crystal structure of fluorite type (Space group: Fm-3m), in which Ce ions are cubic close packed and O ions in the tetrahedron space. Fig. 1, shows the powder XRD pattern. The peaks of all samples were identified and indexed as per JCPDF # 00-034-0394 corresponding to a fluorite- type cubic structure of ceria. CEA and CEC are pure ceria powder at various stock solution of cerium nitrate and fuel ratio.

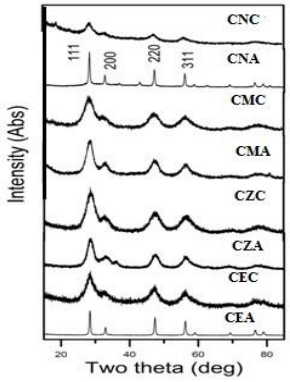

Fig. 1. XRD patterns of samples nitrate

There is no additional peak, which reveals that the material is phase pure ceria. The powders prepared at 0. 25mol of cerium (CEA) show existence of well crystalline and sharp peaks with high intensity counts compared to another (CEC) nitrate fuel ratio compound. In zinc mixed ceria samples, in addition to ceria peaks, some additional peaks were observed in CZA. The additional peaks were identified as hexagonal structure of ZnO (JCPDF #00- 036-1451). But the sample CZC shows single phase of ceria structure because the solubility limit of zinc in ceria is very difficult to find [15]. By totaling Mg, however there was no second peak in XRD pattern due to high solubility of Mg. By mixing nickel a dual phase structure in CNA sample with sharp peak. The additional peaks were identified and indexed for cubic NiO as JCPDF #47-1049. But sample CNC shows the single phase of ceria with broadening of peak, which is due to coherent diffraction grain size as well as arising from the small finite size of the crystallites. Sharpness and broadening of the peaks existing in the samples were attributed to the rate Incorporation of nickel present in the ceria lattice shows in the drastic variation of band gap which is due to concentration of grain boundaries found in SEM images of reaction, reaction temperature, nitrate-fuel ratio and microwave power. Sudden explosion was observed at low concentration of cerium nitrate during preparation, which in turn shows sharp peaks in XRD spectrum. The heating rate of the reaction is the important parameter, which depends on solubility of metal nitrates, fuel ratio and microwave power. Milder reaction affects nucleation rate.

The crystallite size was calculated using Debye-Scherer formula and the lattice parameter was calculated by UNITCELL powder code method. Crystallite size was ranged from 27 nm to 3 nm. These values were listed in Table 1. In pure ceria sample the powder prepared from the lowest nitrate/fuel ratio lattice parameter was very close to the standard ceria lattice parameter. The higher cerium nitrate/fuel ratio composition powder was found to be higher lattice parameter value may be due to the oxygen vacancies or excess of fuel ratio present during preparation or the method of preparation. In Zn, Mg and Ni substituted ceria samples shows the lattice shrinkage. This may be due to the substitution of Ce atoms by Zn, Mg and Ni atoms. In this study fuel ratio and mixing materials plays a vital role for changing micro structural parameters.

The crystallite size of the nanoparticles will alter the optical properties, which were observed in Fig. 2. The mixing with the materials has shifted the absorption position of the ceria to the near visible region. The shifting of the absorption limit to a higher wavelength by mixed materials indicates a modification of the electronic band structure of the doped ceria. It has been already discovered that normally the band gap value decreased slightly for the material prepared using microwave combustion method. Earlier studies showed that the large band gap reduction is possible only excessively increased the concentration of added materials. For all the samples, it was found that absorption wavelength was in the range of 400 nm to 500 nm.

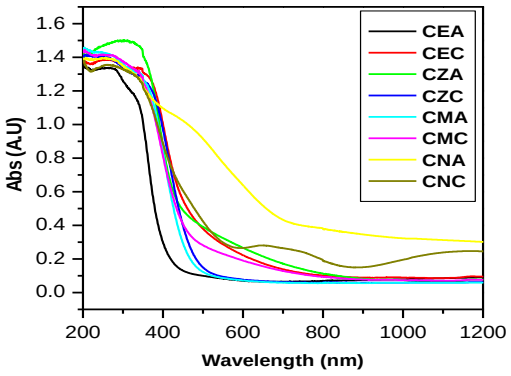

Fig. 2. UV-Vis spectra of samples

This indicates that the modification of electronic band structure of ceria depends on the nature of mixture, concentration of mixture and reaction conditions. The band gap values were calculated via cutoff frequencies shown in Table 1. Lower concentration of the cerium nitrate prepared samples shown the band gap values which are similar to the reported value of pure ceria. The higher concentration of cerium nitrate used for preparation of the samples show decrease in the band gap was due to the concentration of grain boundaries or surface atoms [16].

Table 1. Microstructure, optical and magnetic parameters of ceria samples

S.No	Sample	Crystallite size, nm	Lattice parameter, A°	Band gap energy, eV	Magnetic Saturation M_S, emu	Coercivity H_C, G	Retentivity M_r,emu	M_r/M_s
1	CEA	25.1	5.4165	2.72	139.72E-6	423.73	43.42 E-6	0.3
2	CEC	3.5	5.4479	2.58	3.805 E-3	431.29	162.3 E-6	0.04
3	CZA	3.7	5.3999(2)	2.69	87.06E-6	31.86	8.77E-6	0.1
4	CZC	3.1	5.3730(2)	2.58	1.025E-3	477.1	48.03E-6	0.04
5	CMA	4.0	5.3802(2)	2.93	358.7 E-6	580.46	35.49 E -6	0.098
6	CMC	2.9	5.3832(2)	2.75	958.7 E-6	401.71	58.41 E-6	0.06
7	CNA	27.06	5.4089(1)	3.1	1.8416E-3	474.15	60.571E-6	0.033
8	CNC	3.83	5.4014(3)	1.55	5.6645E-3	414.77	128.29E-6	0.023

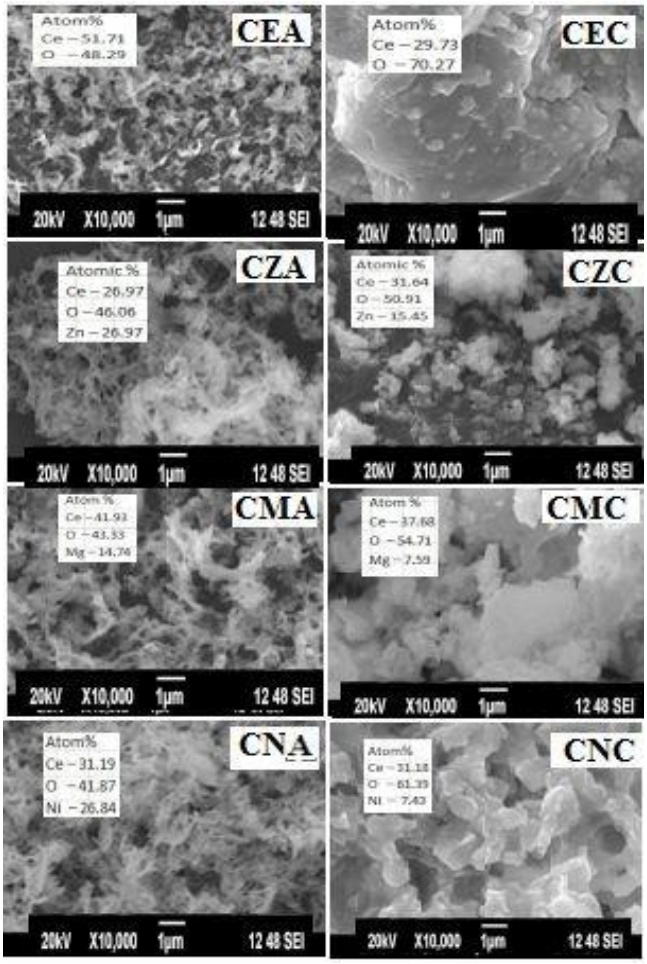

Fig. 3. SEM images and EDAX data of samples

The band gap values show the concentration of Ni dispersed on ceria lattice. During preparation method, the metal nitrates are impregnated into the polymeric product and the gel ignited. The rapid expulsion of a gas during the process of preparation caused the pore formation and leads to localized heating in the polymeric metal nitrate- fuel network. The strong sticky and adhesive force in the gel network improved the inter-particle sticking in the nanoparticles led to loosely packed or agglomerated morphology, which is shown in Fig. 3. The powders have squishy and collapse morphologies depending upon the process of preparation. The TEM images and selected area diffraction pattern shown in Fig. 4, is index to polycrystalline in the fluorite structure and no line corresponding to Mg or Zn or Ni or any other corresponding oxides were detected in CEC, CZC, CMC and CNC samples.

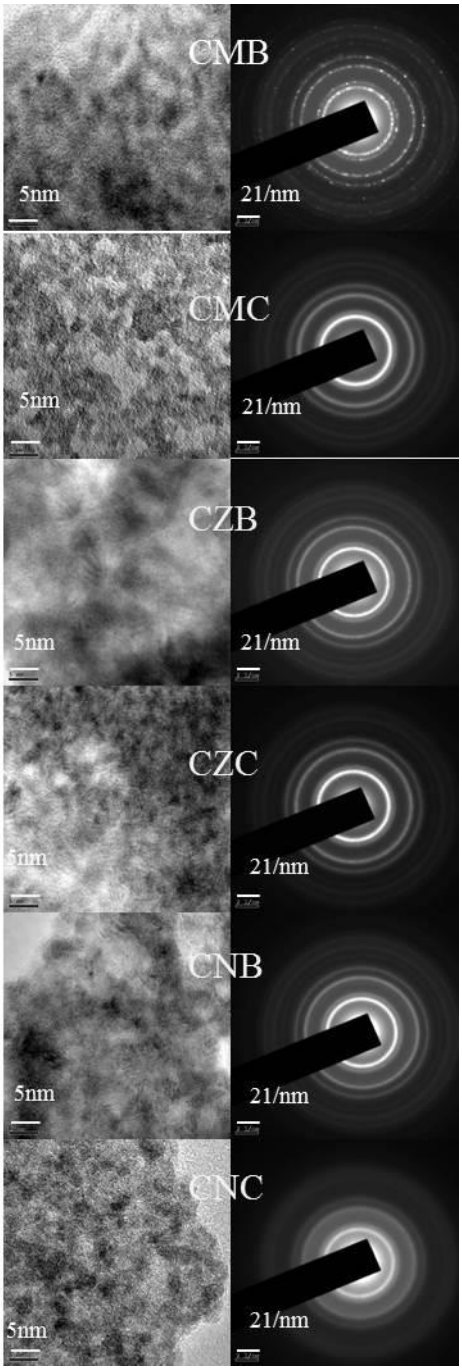

Fig. 4. TEM images and SAED pattern of samples

This again suggests that dispersion of mixed materials on ceria surface. Moderately agglomerated particles seem to be present, which is greatly related to the large surface energy of the nanoparticles. Ceria powders prepared under all conditions lead to the formation of particle agglomerates due to van der Waals forces responsible for the formation of ultra fine ceria particles.

Magnetic hysteresis loops were traced out at room temperature using Vibrating sample magnetometer (VSM) for all synthesized samples of pure and material mixed ceria nanocrystalline powder shown in Fig. 5.

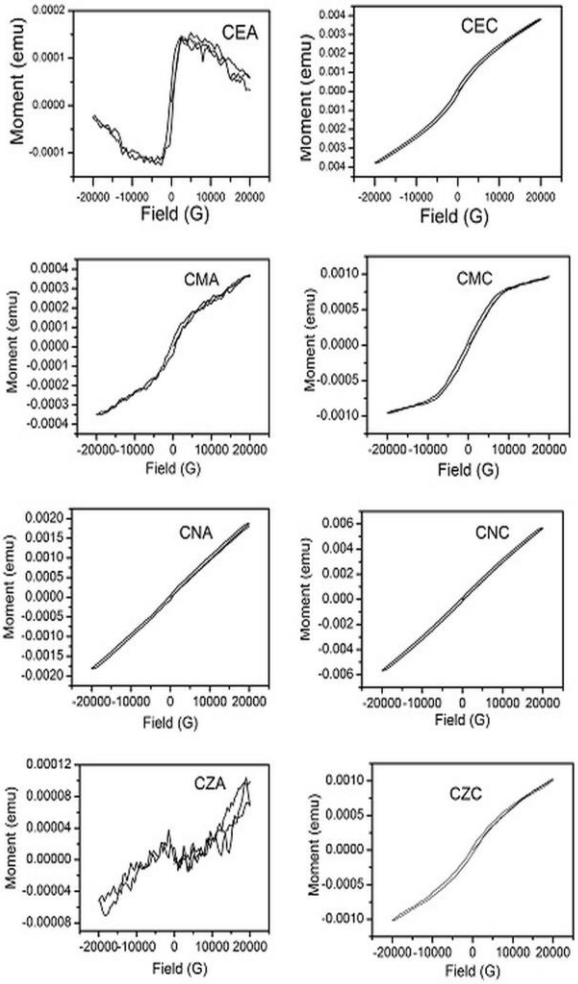

Fig. 5. Magnetic curves of samples

The magnetic parameters were tabulated in Table 1. The loop for CEA clearly shows that ferromagnetic nature of sample which is due to oxygen vacancies created in the structure of pure ceria. There may be exchange interaction between unpaired electrons spins arising from oxygen vacancies formed at surface of nanoparticles. From saturation point the curve behave like diamagnetic substances. This mixed behavior was already reported in literature [17].

The highest saturation to remanence ratio of this sample shows the indication of weak interaction between particles. The sample prepared with 32.5 gm of $Ce(NO_3)_3{\cdot}6H_2O$ exhibits weak ferromagnetic nature and slightly tending to paramagnetic behavior. In addition, the coercive field for CEC is smaller than the sample CEA. This is due to the decreasing of coercive field for reducing particle size after the critical size of the nanoparticle having single magnetic domain. After the critical size, the ferromagnetic effect would become superparamagnetics because of the domination of thermal energy than the magnetostatic energy. The reducing particle size is in well agreement with the result of the X-ray diffraction (Fig. 1, CEA & CEC).

For Zn mixed ceria (CZC), the sample behaviour is close to complete paramagnetic. The biphase structure of the CZA (ceria phase as well as ZnO phase shown in XRD) shows the weak ferromagnetic nature because the interaction between the particles was very weak which shows in remance ratio as well as low value of magnetic saturation The samples CMA and CMC are showing weak ferromagnetic nature, but the saturation magnetization, M_s, for CMC is higher than CMA. The high concentration of Ce^{3+} in CMC may create more defects on the samples, which presume more coupling between the Ce ions, leading to an increase in M_s. For CNA and CNC, the hysteresis measurements indicate that the particles behave only like paramagnetic. Certain amount of Ni ions remains in the interstitial sites too. These isolated Ni ions are not magnetically ordered, which can bring about paramagnetic behavior. The same result is shown in cobalt doped ceria, which implies an important correlation between oxygen vacancies and cobalt doping [18]. This indicates that the ionic Co has a paramagnetic contribution and no ferromagnetic behavior is detected. The interparticle interaction is very weak in CEA, CZA & CMA but strong in CEC, CZC, CMC, CNA & CNC samples.

4. CONCLUSIONS

Pure and ceria based materials are successfully prepared by microwave induced combustion method. The main advantage of the introduction of microwaves into the reaction system is in obtaining a tremendously quick kinetic for crystallization, which may be ascribed to the controlled superheating of the solutions under microwave heating. XRD was used to study the phase and crystal structure. The size and lattice parameter were calculated and analyzed. Lattice shrinkage was observed in the substituted ceria materials, which indicate that the mixed materials are present in the ceria lattice. The microstructural parameter of ceria was affected by the integrated materials and the method of preparation. Optical parameters were drastically affected by the concentration of materials added, grain boundaries and surface atoms which is matched with SEM images. The magnetic curve and parameters were discussed. The magnetic nature of the ceria nanocrystalline materials depends on the mixed materials and also oxygen vacancies. The magnetic saturation and coercive field were increased for the reduced crystallite size except in zinc mixed ceria material due to the complicated alloying situation of zinc ion in ceria.

REFERENCES

1. **De Marzi, L., Monaco, A., De Lapuente, J., Ramos, D., Borras, M., Di Gioacchino, M., Santucci, S., Poma, A.** Cytotoxicity and Genotoxicity of Ceria Nanoparticles on Different Cell Lines in Vitro *International Journal of Molecular Science* 14 2013: pp. 3065 – 3077.

2. **Luengnaruemitchai, A., Osuwan, S., Gulari, E.** Comparative Studies of Low-Temperature Water–Gas Shift Reaction over Pt/CeO_2, Au/CeO_2, and Au/Fe_2O_3 catalysts *Catalysis Communications* 4 2003: pp. 215 – 221.
3. **Miyashita, T.** The Industrial Necessity of Leakage Current Verification Using Sm Doped Ceria Electrolytes in SOFCs and Future Applications *The Open Materials Science Journal* 3 2009: pp. 56 – 61.
4. **Ranga Rao, G., Braja, G.M.** Structural, Redox and Catalytic Chemistry of Ceria Based Materials *Bulletin of the Catalysis Society of India* 2 2003: pp. 122 – 134.
5. **Liu, Z., Ding, D., Liu, M., Ding, X., Chang Chen, D., Li, X., Xia, C., Liu, M.** High-Performance, Ceria-Based Solid Oxide Fuel Cells Fabricated at Low Temperatures *Journal of Power Sources* 241 2013: pp. 454 – 459.
6. **Luo, J., Zha, G., Wang, K., Meng, F.** Research Progress of Origin of Ferromagnetic in Nanoparticle CeO_2 *Advances in Condensed Matter Physics* 2 2013: pp. 1 – 4.
7. **Yabe, S., Yamashita, M., Momose, S., Tahira, K., Yoshida, S., Li, R., Yin, S., Sato, T.** Synthesis and UV-shielding Properties of Metal Oxide Doped Ceria via Soft Solution Chemical Process *International Journal of Inorganic Materials* 3 2001: pp. 1003 – 1008.
8. **Prestgard, M.C., Siegel, G.P., Tiwari, A.** Oxides for Spintronics: A Review of Engineered Materials for Spin Injection *Advanced Materials Letters* 5 (5) 2014: pp. 242 – 247.
9. **Samiha, T. Bishay.** Optimization of Electrical and Magnetic Behaviour of Nanosized $Mn_{0.45}Ce_xFe_{2.55-x}O_4$ *Egyptian Journal of Solids* 32 2009: pp. 31 – 44.
10. **Lubna, R., Shah Ali, B., Zhu, H., Wang, W.G., Song, Y.Q., Zhang, H.W., Shah, S.I., Xiao, J.Q**. Detailed Study on the Role of Oxygen Vacancies in Structural, Magnetic and Transport Behavior of Magnetic Insulator: $Co–CeO_2$ *Journal of Physics- Condensed Matter* 21 2009: pp. 486004 – 486012.
11. **Phokha, S., Pinitsoontorn, S., Maensiri, S.** Structure and Magnetic Properties of Monodisperse Fe^{3+}-doped CeO_2 Nanospheres *Nano-Micro Letters* 5 (4) 2013: pp. 223 – 233.
12. **Maensiri, S., Phokha, S., Laokul, P., Seraphin, S.** Room temperature Ferromagnetism in Fe-doped CeO_2 Nanoparticles *Journal of Nanoscience Nanotechnogy* 9 2009: pp. 6415 – 6420.
13. **Naidu, V., Kandu Sahib, A., Suganthi, M., Prakash, C.** Study of Electrical and Magnetic Properties in Nano Sized Ce-Gd Doped Magnesium Ferrite *International Journal of Computer Applications* 27 2011: pp. 40 – 45.
14. **Kumar, S., Kim, Y.J., Koo, B.H., Lee, C.G.** Structural and Magnetic properties of Ni doped CeO_2 Nanoparticles *Journal of Nanoscience and Nanotechnologies* 11 (11) 2010: pp. 641 – 773.
15. **Ruixing, L., Yabe, S., Yamashita, M., Momose, S., Yoshida, S., Yin, S., Sato, T.** UV-shielding Properties of Zinc Oxide-doped Ceria Fine Powders Derived via Soft Solution Chemical Routes *Materials Chemistry and Physics* 75 2002: pp. 39 – 44.
16. **Ansari, S.A., Khan, M.M., Ansari, M.O., Kalathil, S., Lee, J., Cho, M.H.** Band Gap Engineering of CeO_2 Nanostructure using an Electrochemically active Bioflim for Visible Light Applications *Royal Society of Chemistry Advances* 4 2014: pp. 16782 – 16791.
17. **Phokha, S., Pinitsoontorn, S., ChirawatkuL, P., Poo-Arporn, Y., Maensiri, S.** Synthesis, Characterization, and Magnetic properties of Monodisperse CeO_2 Nanospheres prepared by PVP-assisted Hydrothermal Method *Nanoscale Research Letters* 7 2012: pp. 425 – 438.
18. **Bouaine, A., Green, R.J., Colis, S., Bazylewski, P., Chang, G.S., Moewes, A., Kurmaev, E.Z., Dinia, A**. Appearance of Ferromagnetism in Co-Doped CeO_2 Diluted Magnetic Semiconductors Prepared by Solid-State Reaction *Journal of Physical Chemistry C* 115 2011: pp. 1556 – 1560.